

Synthesis, characterization, and biological significance of mixed ligand Schiff base and alizarin dye-metal complexes

Laith Jumaah Al-Gburi[★] and Taghreed H. Al-Noor

Department of Chemistry, College of Education for Pure Sciences – Ibn Al-Haitham, University of Baghdad, Iraq

(Received May 24, 2023; Revised August 9, 2023; Accepted August 30, 2023)

Abstract: This study reports the synthesis of a bi-dentate Schiff base ligand (L), 7-(2-((2-formylbenzylidene) amino)-2-phenylacetamido)-3-methyl-8-oxo-5-thia-1-azabicyclo[4.2.0]oct-2-ene-2-carboxylic acid, prepared from phthalaldehyde and cephalixin antibiotic. The synthesized Schiff base ligand (L) and the secondary ligand alizarin (Az) are used to prepare the new complexes $[M(Az)_2(L)]$ and $[Cr(Az)_2(L)]Cl$, where $M = Mn(II), Co(II), Ni(II), Cu(II),$ and $Zn(II)$. The mode of bonding of the Schiff base has been characterized by UV-Visible, FT-IR, Mass, $^1H-$, and $^{13}C-NMR$ spectroscopic techniques, and micro elemental analysis (CHNS). The complexes were characterized using UV-Vis, FT-IR, molar conductance, magnetic moment, and thermal analysis (TG/DTG). The molar conductance data revealed that the complexes are non-electrolytes except for $[Cr(L)(Az)_2]Cl$, which is an electrolytic type 1:1. The Schiff base and its complexes have been tested for their biological activity against two strains of bacteria and one fungus. When screened against gram-positive and gram-negative pathogens, the Az and L ligands and their complexes showed potential antimicrobial activity.

Key words: synthesis, schiff base, cephalixin, biological activity, metal-complexes

1. Introduction

Schiff base and alizarin dye ligands are a class of compounds extensively used as indicators in analytical chemistry and in organometallic chemistry. Cephalixin is an antibiotic compound that represents the first generation of cephalosporin, which possesses excellent biological activity in terms of its effectiveness against gram-positive and moderate response against gram-negative strains of bacterial pathogens.¹ The chemical structure of cephalixin, when it links to metal ions, shows that the α -amino moiety of the acyl group is

involved in the linkage, as proposed by many researchers.²⁻⁴ Anacona *et al.*³ synthesized a Schiff base, which is a derivative of sulphathiazole and cephalixin, to be used later as a ligand for metal complexes with the chemical formula $[ML(OAc)(H_2O)_2]$ as well as a copper(II) complex as trinuclear with the chemical formula $[Cu_3L(OH)_5]$. Jeliński and Cysewski⁴ investigated the color and structures of alizarin in the form of complexes with alkali metals using computational and quantum calculation methods in methanol solution. Wang *et al.*⁵ investigated the anti-amyloid effects of alizarin and 1,2,4-trihydroxyanthraquinone (purpurin),

[★] Corresponding author

Phone : +96401-778-7086

E-mail : laith.jumaa1105a@ihcoedu.uobaghdad.edu.iq

This is an open access article distributed under the terms of the Creative Commons Attribution Non-Commercial License (<http://creativecommons.org/licenses/by-nc/3.0>) which permits unrestricted non-commercial use, distribution, and reproduction in any medium, provided the original work is properly cited.

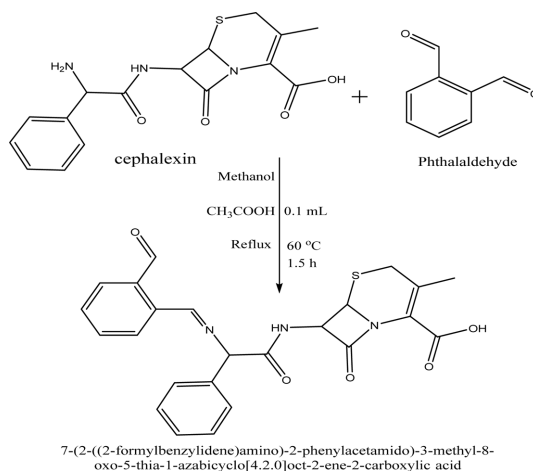
reporting high bioactive compounds and their anti-oxidant, antitumor, and antibacterial activity.

Many researchers have investigated the activity of alizarin as a radical scavenger from the thermodynamic and conformational behavior perspective by employing quantum computation carried out in water solution and gas phase.⁶⁻⁸ The coordination with suitable metal ions leads to some medical applications, such as antitubercular activity.⁹⁻¹¹ In this article, we focus on the production of Schiff bases (L) derived from phthalaldehyde and cephalixin antibiotic, and their treatment with Mn(II), Co(II), Ni(II), Cu(II), and Zn(II). The aim of this paper is to study the thermal stability and antimicrobial effects of synthesized mixed ligand Schiff base and alizarin dye-metal complexes.

2. Experimental Section

2.1. Materials and methods

UV-Vis spectral data in DMSO (10^{-3} M) were recorded on a Shimadzu UV-160A Ultraviolet Visible Spectrophotometer. FTIR was reported on a Shimadzu FTIR-8400S Fourier Transform Infrared Spectrometer ($400 - 4000 \text{ cm}^{-1}$) with samples prepared in the form of KBr discs. Atomic absorption was obtained using a Shimadzu A.A-160A, while the conductance was measured for (10^{-3} M) complexes in DMSO using a Philips PW-Digital Conduct meter. Magnetic properties were performed using an Auto Magnetic Susceptibility Balance Sherwood Scientific Instrument. In addition, melting points were obtained using a Melting Point Apparatus. Cephalixin, alizarin, cobaltous chloride hexahydrate 98.8 %, nickel chloride hexahydrate 99.9 %, copper chloride dihydrate 98 %, and zinc



Scheme 1. Synthesis route of the Schiff base ligand (L).

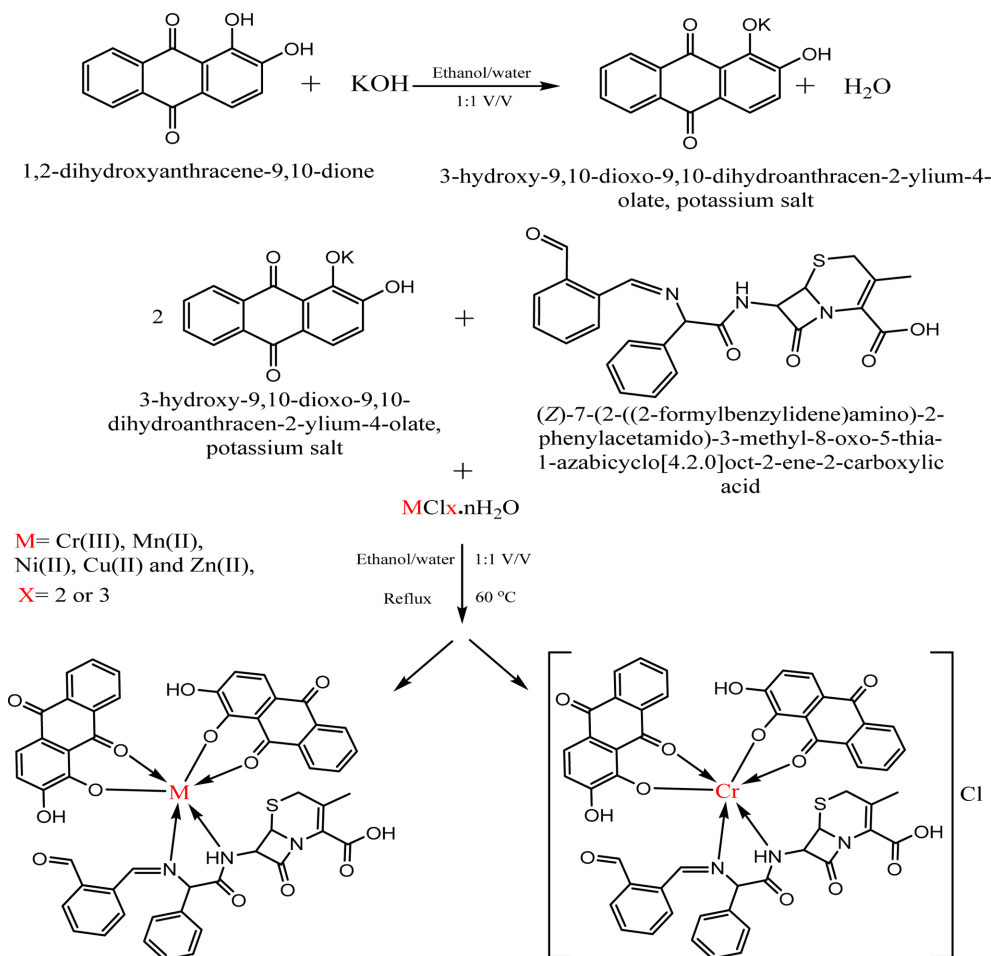
chloride 98.8 % (Merck) were used as received from the suppliers.

2.2. Synthesis of Schiff base ligand

In a 100 mL flask, the Schiff base ligand (L^1) was prepared by a condensation reaction between phthalaldehyde and cephalixin compounds. Phthalaldehyde (3 mmol, 0.402 g) was dissolved in 25 mL of methanol, and cephalixin (3 mmol, 1.042 g) was dissolved in 30 mL of methanol. Then, 0.1 mL of acetic acid was added to the mixture with constant stirring. Under controlled conditions, the reaction mixture was heated to 60°C and subjected to reflux for 1.5 hours. Throughout the reflux process, TLC was used to monitor the progress of the reaction until its completion (Scheme 3 – 1). The yellow precipitated compound was filtered, washed with hot methanol, recrystallized to obtain a pure sample, and dried in CaCl_2 (Yield: 89 %) (Table 1).

Table 1. Physical properties and microanalysis results for L and Ceph ligands

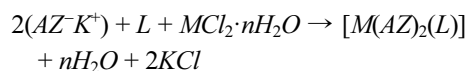
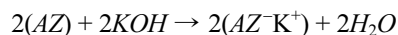
Compound formula	Molecular weight (g/mol)	Melting point temperature ($^\circ\text{C}$)	Color	Theoretical (Experimental)			
				C%	H%	N%	S%
Cephalixin Ceph $\text{C}_{16}\text{H}_{17}\text{N}_3\text{O}_4\text{S}$	365.00	326	Creamy	52.6	5.2	11.5	8.78
Schiff base (L) $\text{C}_{24}\text{H}_{21}\text{N}_3\text{O}_5\text{S}$	463.50	120–122	Orange	62.19 (61.01)	4.57 (4.81)	9.07 (9.1)	6.92 (6.40)



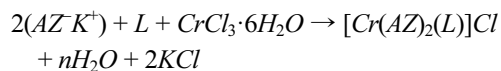
Scheme 2. Synthesis route of the metal (II) and Cr(III) complexes.

2.3. Synthesis of metal complexes

All the complexes were synthesized using the method illustrated in Scheme 1. Generally, the complexes were prepared by reacting the respective metal chloride MCl₂·nH₂O and CrCl₃·6H₂O at room temperature in an ethanol/water (1:1 v/v) solvent with the ligands using a [L:M:2AZ] (1:1:2) mole ratio. Specifically, one mole of Schiff base (L) (0.463 g), one mole of metal chloride, and two moles of mono potassium salts of alizarin (AZ^{-K⁺}) (0.48 g) were used as a base, after adding KOH to the alizarin (C₁₄H₈O₄). Pure complexes formed only at pH 7–8, as shown in the following equations:



where $n = 0 \dots 6$, and M = Mn(II), Co(II), Ni(II), Cu(II), and Zn(II)

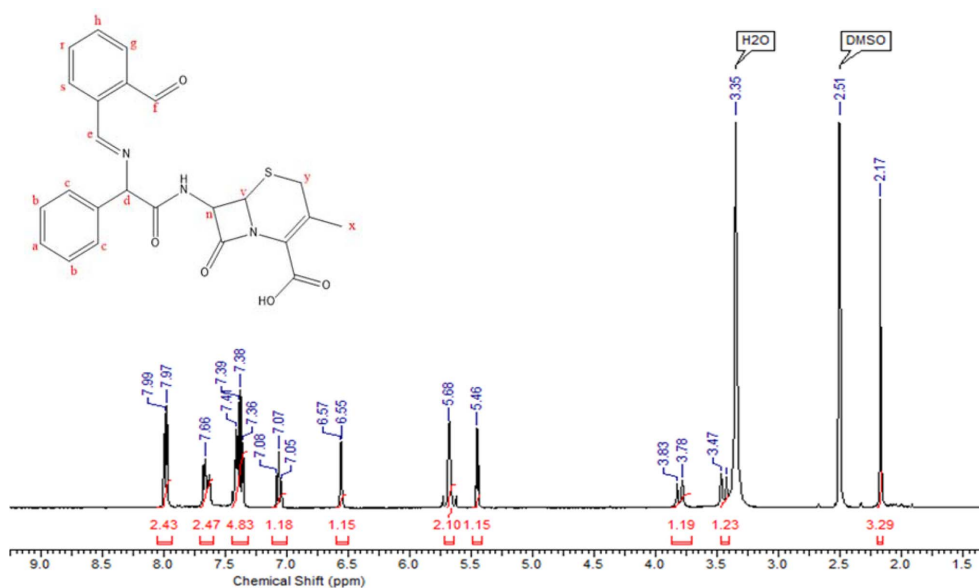


3. Results and Discussion

The orange-colored Schiff base ligand (L), with a molecular formula of C₂₄H₂₁N₃O₅S and a molecular

Table 2. Analytical data and some physical characteristics of $[M(AZ)_2(L)]$ complexes

Compounds	Molecular weight	Color	Melting point °C	Λ_m DMSO 10^{-3} M (μScm^{-1})	M% found (Calc.)
$[\text{Cr}(\text{AZ})_2(\text{L})]\text{Cl}$	993.91	Reddish Yellow	>250	25.42	6.01 (5.23)
$[\text{Mn}(\text{AZ})_2(\text{L})]$	996.85	Dark Brown	>250	3.68	6.14 (5.51)
$[\text{Ni}(\text{AZ})_2(\text{L})]$	1000.61	Dark Brown-Blue	>250	2.39	6.19 (5.87)
$[\text{Cu}(\text{AZ})_2(\text{L})]$	1005.46	Dark Brown	>250	2.62	7.00 (6.32)
$[\text{Zn}(\text{AZ})_2(\text{L})]$	1007.30	Reddish Brown	>250	1.16	7.70 (6.49)

Fig. 1. $^1\text{H-NMR}$ spectrum of the prepared Schiff base ligand (L).

weight of 463.508 g/mol, was obtained and characterized by elemental CHN analysis. Elemental analyses for M% and (CHN)% were found to be in agreement with the proposed molecular formula of the complexes. All complexes are insoluble in water but soluble in common organic solvents. The molar conductance Λ_m (1×10^{-3} M, DMSO) is 1.16–3.68 $\text{ohm}^{-1}\cdot\text{cm}^2\cdot\text{mol}^{-1}$ for $[\text{M}(\text{AZ})_2(\text{L})]$, which exhibits a non-electrolytic nature, while it is 25.42 $\text{ohm}^{-1}\cdot\text{cm}^2\cdot\text{mol}^{-1}$ for $[\text{Cr}(\text{AZ})_2(\text{L})]\text{Cl}$, which exhibit an electrolytic nature with a type 1:1 ratio.¹² The test for chloride ions using AgNO_3 solution was negative for all M(II) complexes except for $[\text{Cr}(\text{AZ})_2(\text{L})]\text{Cl}$, which was positive, indicating that Cl ions are outside the coordination sphere of the Cr(III) complex. The above complexes are soluble in concentrated hydrochloric acid and in most organic solvents except for benzene. The analytical

and some physical data are listed in Table 2.

3.1. $^1\text{H-NMR}$ and $^{13}\text{C-NMR}$ Spectra

The $^1\text{H-NMR}$ spectrum of Schiff base (L) (recorded in ppm d^6 -DMSO, 400 MHz) (Fig. 1) supports its structure. It exhibits a singlet resonance at 13.37 ppm δ (s, 1H, OH), 8.00 ppm δ (s, 1H, CfH), 7.98 ppm δ (s, 1H, CeH), a multiplet in the region from 6.56 to 7.67 ppm δ (m, 1H, CaH, CbH, CcH, CsH, CrH, ChH, CgH), 5.69 ppm δ (s, 2H, CyH), 5.46 ppm δ (s, 1H, CdH), 3.83 and 3.79 ppm δ (d, 1H, CnH), 3.47 and 3.43 ppm δ (d, 1H, CvH), and 2.17 ppm δ (s, 3H, CxH).^{13,14}

The $^{13}\text{C-NMR}$ spectrum of (L) is shown in Fig. 2, which exhibits peaks as follows: $\delta\text{C}_k = 163$ ppm, $\delta\text{C}_z = 161$ ppm, $\delta\text{C}_e = 155$ ppm, $\delta\text{C}_w = 141$ ppm, $\delta\text{C}_{a,b,c,f,s,r,h,g,m,t,p,u} = 101 - 133$ ppm, $\delta\text{C}_d = 60$ ppm,

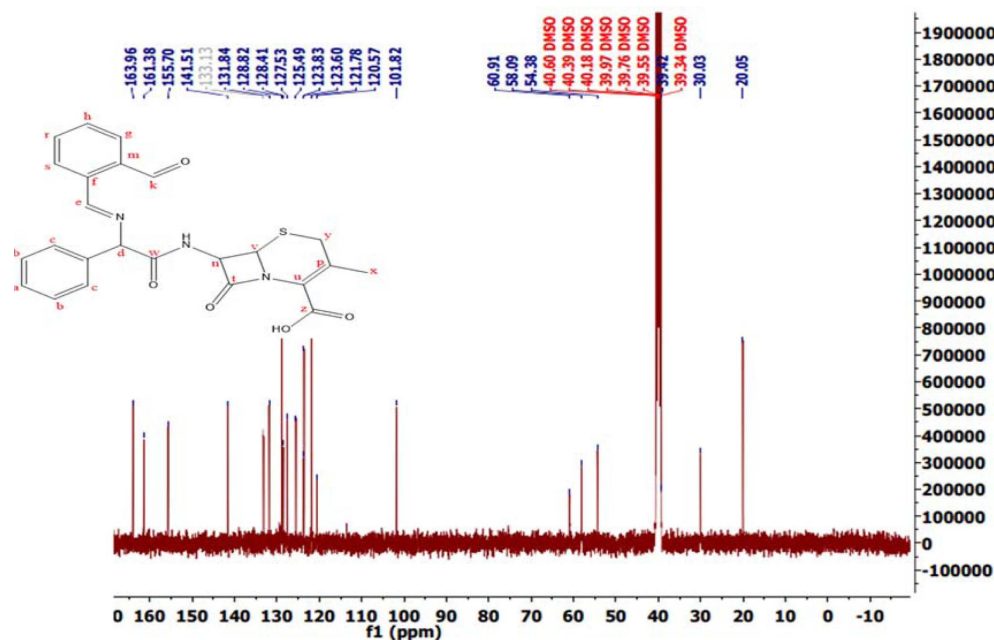


Fig. 2. ¹³C-NMR spectrum of the prepared Schiff base ligand (L).

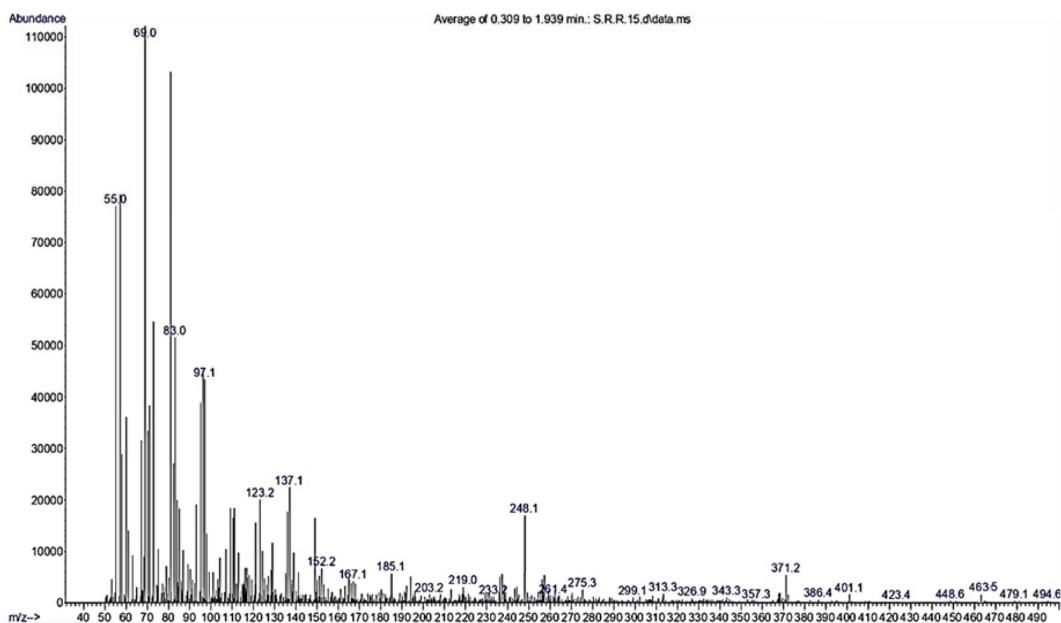


Fig. 3. Mass spectrum of the prepared Schiff base [L].

$\delta C_v = 58$ ppm, $\delta C_n = 54$ ppm, $\delta C_y = 30$ ppm, and $\delta C_x = 20$ ppm.^{13,15}

3.2. Mass spectrum of the ligand [L]

The mass spectrum of the synthesized Ligand (L)

is displayed in Fig. 3. The spectrum revealed several fragmentations centered at M/Z values. The parent ion peak [M⁺] was observed at a mass-to-charge ratio of 463.5 (m/z), corresponding to the molecular weight of the Schiff base [C₂₄H₂₁N₃O₅S]⁺, thus

confirming the proposed formula. Additionally, the presence of other fragments, their relative abundances, and the fragmentation pathways are depicted in

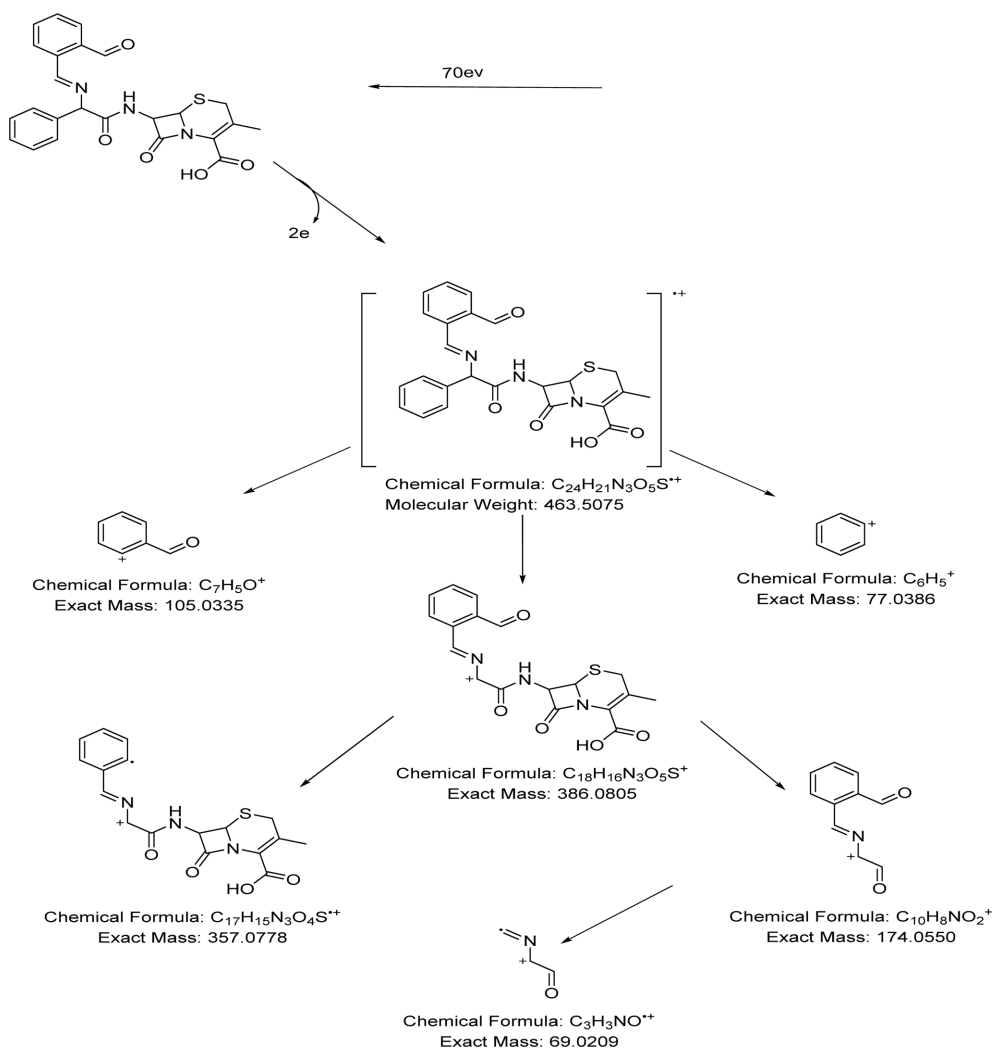
Table 3. Suggested molecular fragments of the mass spectrum of the Schiff base [L]

M.wt	Format
463.50	$[C_{24}H_{21}N_3O_5S]^+$
386.08	$[C_{18}H_{16}N_3O_5S]^+$
357.07	$[C_{17}H_{15}N_3O_4S]^+$
174.05	$[C_{10}H_8NO_2]^+$
105.03	$[C_7H_5O]^+$
77.03	$[C_6H_5]^+$
69.02	$[C_3H_3NO]^+$

Scheme 3 and summarized in Table 3, providing strong evidence for the formation and structure of the Schiff base ligand.^{4,12}

3.3. Thermal analysis TGA

The ligand L remains stable until around 60 °C, after which it starts to melt and subsequently decomposes at 258 °C, losing 7–8 % of its mass by weight corresponding to the release of the C=N-C group or CO₂ molecules (38 g/mol). The second mass loss of 31 %, equivalent to 144 g/mol of L, occurs between 91 % and 60 % weight, corresponding to the decomposition of the C₆H₈N₂S group. The third mass loss of 17 %,



Scheme 3. Proposed fragmentation sequence of the prepared Schiff base (L).

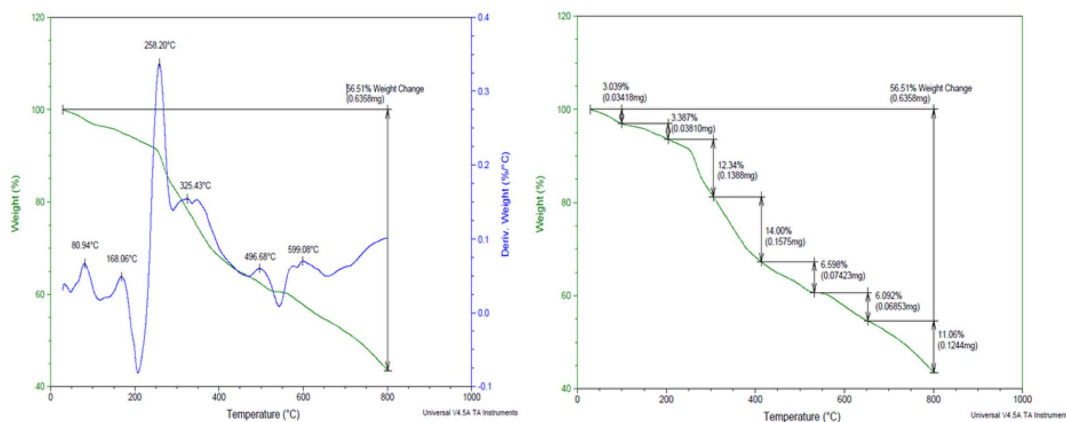
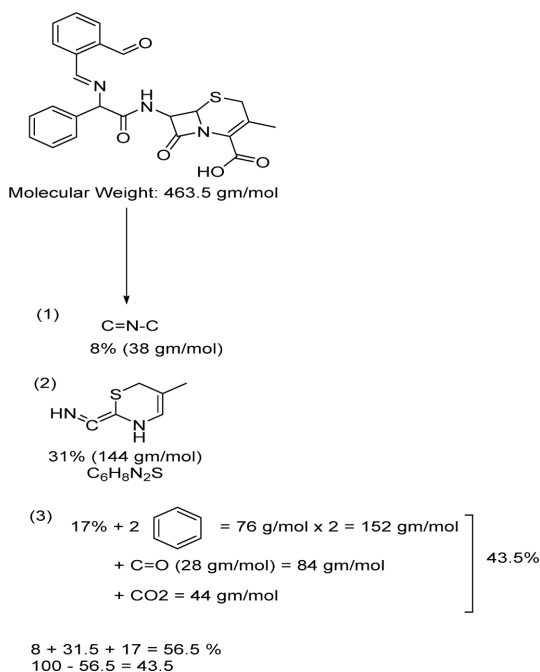


Fig. 4. TG/DTG curve of the prepared Schiff base ligand (L).

Table 4. Summarized results of the thermal analysis of the prepared Schiff base ligand (L)

Compound	first mass losing % = formula weight (g/mole)	Temp. °C	Second mass losing % = ligand formula (g/mole)	Temp. °C	Third mass losing % = ligand formula (g/mole)	Temp. °C
L	8% = 14 (g/mole) = C=N-C fragment or CO ₂ molecules	60	31% = 38 (g/mole) = C ₆ H ₈ N ₂ S group	258	17% = 76 (g/mole) = C ₆ H ₅ group	560



Scheme 4. Proposed TGA thermal degradation behavior of the prepared Schiff base ligand.

equivalent to 76 g/mol of L, occurs between 60 % and 43 % weight, corresponding to the decomposition

of the C₆H₅ group. The total weight loss is 56.5 % of the mass of ligand L (463.5 g/mol), leaving behind 43.5 % (201.6 g/mol) of L's mass, which decomposes into fragments including three molecules of CO and one molecule of CO₂. See Fig. 4 for graphical representation. The results of the TGA measurements are summarized in Table 4.

3.4. Fourier transform infrared analysis

The Fourier Transform Infrared Analysis (FTIR) spectrum of the starting material cephalixin exhibits a band at 3,275 cm⁻¹ due to ν(N-H) primary amine stretching vibration.¹⁶ Bands at 3,219 cm⁻¹ and 3,049 cm⁻¹ are attributed to ν(N-H) secondary amine stretching vibrations. The COO⁻ group of cephalixin shows strong absorptions at 1,759 cm⁻¹ for ν(C=O) and 3,406 cm⁻¹ for ν(O-H) stretching, with 1,595 cm⁻¹ and 1,398 cm⁻¹ representing the asymmetrical and symmetrical stretching of the COO⁻ group, respectively,^{6,12,17} where Δν = 197 cm⁻¹ [ν_{asym} (COO⁻) - ν_{sym} (COO⁻)]. The band at 1,689 cm⁻¹ corresponds to ν(C=O) for the β-Lactam group.¹⁸ The carbonyl stretching frequencies for the amide, acid, and β-

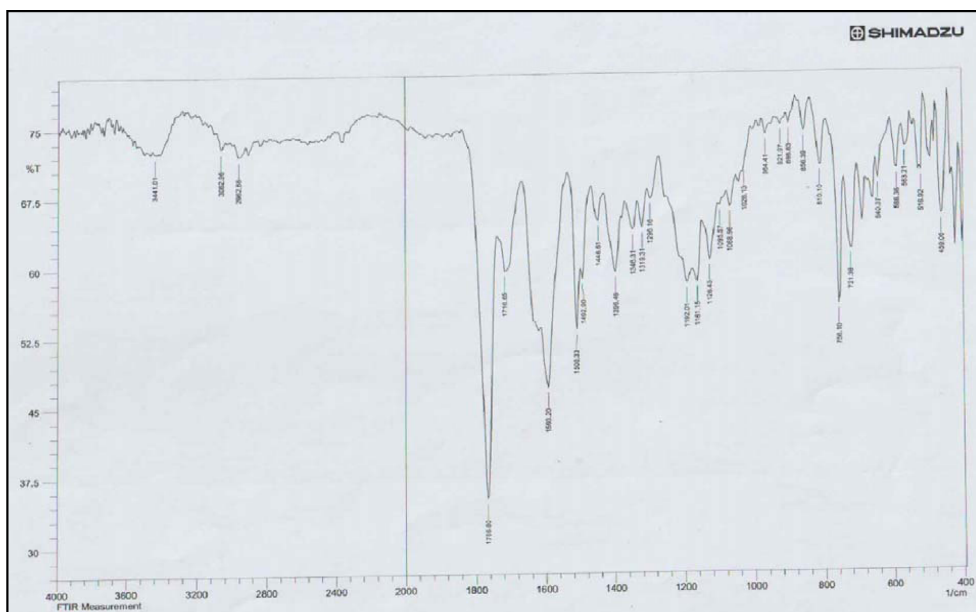


Fig. 5. FTIR spectrum of the prepared Schiff base ligand (L).

Table 4. FTIR spectral data of the ligands and metal complexes

Compound	AZ	Cephalexin	L ¹	[Cr(AZ) ₂ (L ¹)]Cl	[Mn(AZ) ₂ (L ¹)]	[Ni(AZ) ₂ (L ¹)]	[Cu(AZ) ₂ (L ¹)]	[Zn(AZ) ₂ (L ¹)]
O-H	3421, 3371	3466	3441, 3362	3371	3379	3371	3414 3371	3441
$\nu_{\text{asym}}(\text{NH}_2)$, $\nu_{\text{sym}}(\text{NH}_2)$ amine	----	3275, 3219	-	-	-	-	-	-
=C-H Ar.	3074	3010	-	3074	3066	3066	3032	3066
-C-H Aliph.	-----	2976, 2931	2962, 2800	2912, 2846	2916	2919	2870	2971, 2870
>C=O	1662, 1631	s---	-	1662, 1631	1662	1631	1662, 1608	1685, 1631
(>C=C<) anthraquinone	1586, 1450	-	-	1589	1589	1589	1585	1589
C=N	---	1689	1681, 1612	1631	1621	1631	1608	1631
(C-O)	894	---	1296, 898	1265, 894	1261, 498	1284, 894	1284, 894	1284, 894
(C-S)	---	829	810	829	829	825	829	829
(M-O)	---	---	---	563	594	594	563	582
(M-O)	---	---	---	524	524	524	524	524
(M-N)	---	---	---	420	455	418	420	466

Lactam groups in cephalixin's free ligand are observed at $1,595\text{ cm}^{-1}$, $1,759\text{ cm}^{-1}$, and $1,789\text{ cm}^{-1}$, respectively. Additionally, the spectrum shows peaks at $1,577\text{ cm}^{-1}$ and $3,010\text{ cm}^{-1}$ assigned to $\nu(\text{C}=\text{C})$ aromatic, $\nu(\text{C}-\text{H})$ aromatic, respectively. The FTIR spectrum of phthalaldehyde, as a starting material, shows a band at

$1,762\text{ cm}^{-1}$ due to $\nu(\text{C}=\text{O})$. The bands assigned include $\nu(\text{C}-\text{H})$ aromatic at $3,082\text{ cm}^{-1}$, $\nu(\text{C}-\text{H})$ aliphatic at $2,900\text{ cm}^{-1}$, $\nu(\text{C}=\text{C})$ aromatic at $1,685\text{ cm}^{-1}$ and $1,195\text{ cm}^{-1}$, and $\nu(\text{C}-\text{C})$ aliphatic. The IR spectrum of (L) shows peaks at $3,441\text{ cm}^{-1}$ due to the stretching vibration of the OH group. A new band observed at

1,651 cm^{-1} in the free (L) spectrum is assigned to the azomethine group ($-\text{N}=\text{C}-$) of the Schiff base, and at 1,593 cm^{-1} to $\nu(\text{C}=\text{O})$, as well as $\nu(\text{C}=\text{O})$ for the β -Lactam group at 1,766 cm^{-1} .^{19,21} The FTIR spectra of the complexes exhibit three absorption bands in the far-infrared region: 563–594 cm^{-1} , 524 cm^{-1} , and 420–466 cm^{-1} , which can be assigned to (M-O), (M-O), and (M-N) vibrations, respectively. Both ligands in the complexes act as bidentate ligands, forming coordination bonds with the M(II) ion through different chelation groups.

3.5. Magnetic and electronic analysis of the ligand and its complexes

The magnetic moment data and corresponding transitional absorption bands are listed in Table 5. The effective magnetic moments obtained for all complexes corroborate the octahedral geometry of the complexes with electron configurations.²³

The UV-Vis spectrum of (AZ) shows two peaks: 277 nm (36,101 cm^{-1}) assigned to $\pi \rightarrow \pi^*$ transition and 435 nm (22,988 cm^{-1}) assigned to $n \rightarrow \pi^*$ transitions. These peaks correspond to electronic transitions within the organic ligand.¹⁰

The UV-Vis spectrum of (L) (Fig. 6) exhibits three peaks: 265 nm (37,736 cm^{-1}) assigned to $\pi \rightarrow \pi^*$ transition, and 306 nm (32,680 cm^{-1}) and 434 nm (23,041 cm^{-1}) attributed to $n \rightarrow \pi^*$ transitions.^{20,22}

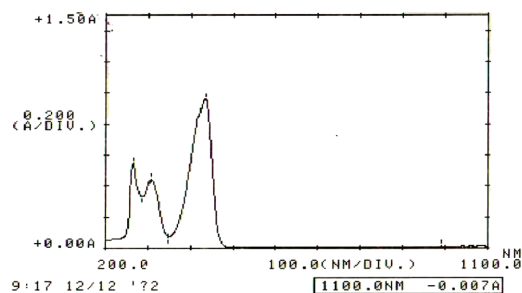


Fig. 6. UV/Vis spectrum of the Schiff base ligand.

The magnetic moment of the $[\text{Mn}(\text{AZ})_2(\text{L})]\text{d}^5$ complex is 5.61 B.M. The UV/Vis absorption spectrum of the $[\text{Mn}(\text{AZ})_2(\text{L})]$ complex displays two intense peaks. The first peak at 270 nm (37,037 cm^{-1}) corresponds to a ligand field (L.F) $n \rightarrow \pi^*$ transition, while the second peak at 527 nm (18,975 cm^{-1}) can be attributed to a charge transfer (C.T) transition. These results confirm the octahedral geometry of this complex and are consistent with data reported by several researchers.^{19,22,23}

The magnetic moment of the $[\text{Ni}(\text{AZ})_2(\text{L})]\text{d}^8$ complex is determined to be 3.65 B.M. The electronic absorption spectrum of the $[\text{Ni}(\text{AZ})_2(\text{L})]$ complex displays two intense peaks. The first peak at 273 nm (36,630 cm^{-1}) corresponds to a L.F $n \rightarrow \pi^*$ transition, while the second peak at 573 nm (17,452 cm^{-1}) can be attributed to a C.T transition.^{24,25}

Table 5. Electronic data and magnetic susceptibility value of the prepared ligand and metal complexes

Compound	λ_{max} nm	ν , cm^{-1}	ϵ_{max} $\text{mol}^{-1} \cdot \text{L} \cdot \text{cm}^{-1}$	Assignments	μ_{eff} B.M
$[\text{Cr}(\text{AZ})_2(\text{L})]\text{Cl}$	265	37,736	546	$\pi \rightarrow \pi^*$	-
	306	32,680	448	$n \rightarrow \pi^*$	
	434	23,041	964	$n \rightarrow \pi^*$	
$[\text{Mn}(\text{AZ})_2(\text{L})]$	271	36,900	2,074	$n \rightarrow \pi^*$ (L.F.)	3.95
	378	26,455	308	Charge transfer	
	438	22,831	474	Charge transfer	
	546	18,315	281	$^4\text{A}_{2g} \rightarrow ^4\text{T}_{1g}(\text{F}) \nu_3$	
$[\text{Ni}(\text{AZ})_2(\text{L})]$	270	37,037	1,547	(L.F) ($n \rightarrow \pi^*$)	5.61
	527	18,975	381	Charge transfer	
$[\text{Cu}(\text{AZ})_2(\text{L})]$	273	36,630	2,114	(L.F) ($n \rightarrow \pi^*$)	3.65
	573	17,452	410	Charge transfer	
$[\text{Zn}(\text{AZ})_2(\text{L})]$	271	36,900	2,172	(L.F) ($n \rightarrow \pi^*$)	1.56
	538	18,587	688	Charge transfer	

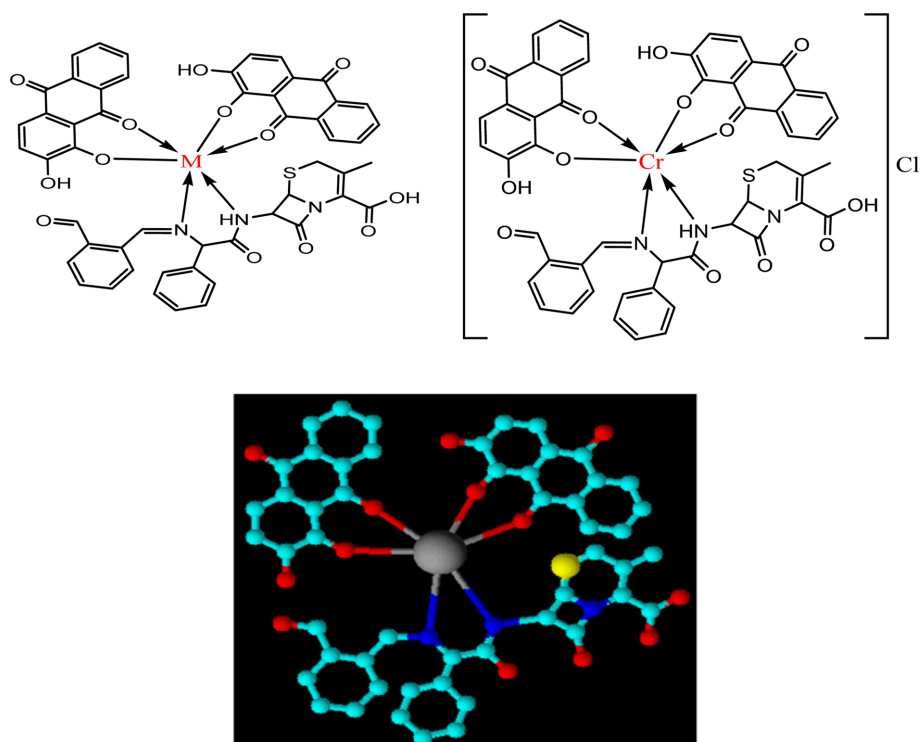


Fig. 7. Suggested octahedral structures of the synthesized complexes.

The magnetic moment of the Cu(II) d^9 is determined to be 1.56 B.M. The UV/Vis spectrum of the $[\text{Cu}(\text{AZ})_2(\text{L})]$ complex exhibits two bands. The first band at 271 nm ($36,900 \text{ cm}^{-1}$) is assigned to the L.F $n \rightarrow \pi^*$ transition. The second band at 538 nm ($18,587 \text{ cm}^{-1}$) is attributed to the charge-transfer intra-ligand transition. These transitions can be explained by the Jahn-Teller effect, indicating a distorted octahedral geometry for the complex.^{26,27}

The UV/Vis spectrum of the $[\text{Zn}(\text{AZ})_2(\text{L})]$ complex exhibits two highly intense peaks: the first at 276 nm ($37,037 \text{ cm}^{-1}$) due to a $\pi \rightarrow \pi^*$ intra-ligand transition, and the second peak at 436 nm ($22,936 \text{ cm}^{-1}$) attributed to the metal-ligand C.T. This is further supported by its diamagnetic nature, characteristic of a d^{10} -complete complex.^{19,28,29}

3.6. Proposed molecular structure for studying complexes

Based on the analysis above, spectral analysis suggests an octahedral geometry for all the prepared

complexes, with a coordination number of six, formulated as $[\text{M}(\text{AZ})_2(\text{L})]$ and $[\text{Cr}(\text{AZ})_2(\text{L})]\text{Cl}$. The general structures of the complexes are depicted in Fig. 7.

3.7. Antimicrobial studies

The *in-vitro* antibacterial and antifungal screening data are presented in Table 6 and illustrated in Figs. 8 and 9. DMSO was used as a neutral control and solvent for the ligands and synthesized complexes.

Table 6. Biological activity zone inhibition (mm) of the ligands and their complexes

Compound	Staphylococcus aureus	Klebsiella pneumonia	Candida albicans
AZ Alizarin	12	14	14
Schiff Base (L)	10	12	12
Control DMSO	-ve	-ve	-ve
$[\text{Cr}(\text{AZ})_2(\text{L})]\text{Cl}$	18	14	12
$[\text{Mn}(\text{AZ})_2(\text{L})]$	15	13	12
$[\text{Ni}(\text{AZ})_2(\text{L})]$	20	15	17
$[\text{Cu}(\text{AZ})_2(\text{L})]$	22	12	12
$[\text{Zn}(\text{AZ})_2(\text{L})]$	22	13	13

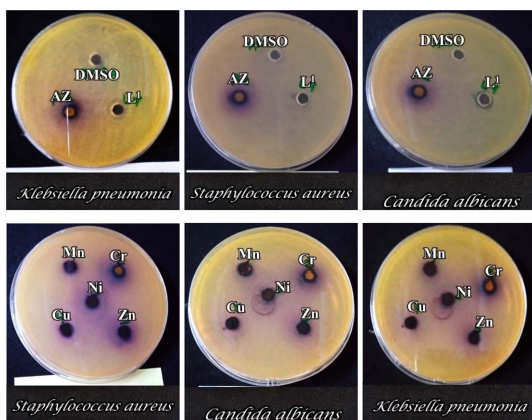


Fig. 8. Plates - Zone of Inhibition (ZI) for antibacterial activity of $[L:M:2AZ]$ compounds.

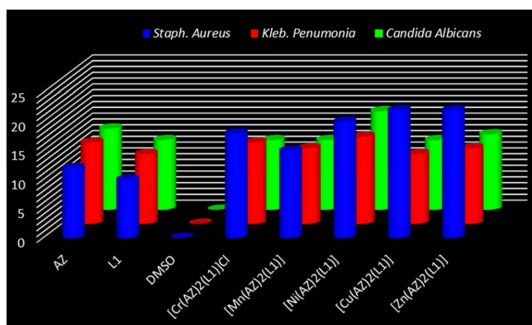


Fig. 9. Inhibition zone for studied complexes against Staphylococcus, Klebsiella, and Candida albicans.

The results indicate that most of the complexes exhibit higher activity compared to the Schiff base alone but are generally less active than the standard drug (Az).

The biologically active $[Ni(AZ)_2(L)]$ complex demonstrated notable antimicrobial and antifungal effects. The $[Zn(AZ)_2(L)]$ complex also exhibited significant antibacterial activity, possibly due to the electrons of its d^{10} orbitals. Both ligand L and DMSO showed moderate inhibitory activity, while the complexes showed substantially higher activity compared to the free Schiff base ligands.^{28,30}

4. Conclusions

This study synthesized and characterized a Schiff base ligand (L) derived from phthalaldehyde and

Cephalexin antibiotic using various spectroscopic techniques (FTIR, UV-Vis, Mass spectra, 1H and ^{13}C NMR Spectra, and thermal analysis). The synthesized ligand, along with the secondary ligand Alizarin (Az), was used to prepare new complexes $[M(L)(AZ)_2]$ and $[Cr(L)(AZ)_2]Cl$, where $M = Mn(II), Ni(II), Cu(II), and Zn(II)$. A molar ratio of 1:1:2 (M:L:AZ) was employed for all complexes. Spectral data indicated that Schiff base (L) acts as a bidentate ligand, coordinating through the carbonyl oxygen atom and azomethine nitrogen atom. *In-vitro* antibacterial and antifungal screening revealed moderate antimicrobial activity for some complexes, suggesting their potential as candidates for further investigation in biomedical applications.

Acknowledgments

The authors are grateful to Baghdad University, Iraq, for supporting this investigation.

References

1. M. S. Sinicropi, J. Ceramella, D. Iacopetta, A. Catalano, A. Mariconda, C. Rosano, C. Saturnino, H. El-Kashef, and P. Longo, *International Journal of Molecular Sciences*, **23**(23), 14840 (2022). <https://doi.org/10.3390/ijms232314840>
2. A. J. A. Al-Sarray, T. Al-Kayat, B. M. Mohammed, M. J. B. Al-assadi, and Y. Abu-Zaid, *Journal of Medicinal and Chemical Sciences*, **5**(7 (Special Issue)), 1321-1330 (2022). <https://doi.org/10.26655/JMCHEMSCI.2022.7.21>
3. J. Anaconda, J. L. Rodriguez, and J. Camus, *Spectrochimica Acta Part A: Molecular and Biomolecular Spectroscopy*, **129**, 96-102 (2014). <https://doi.org/10.1016/j.saa.2014.03.019>
4. T. Jeliński and P. Cysewski, *Journal of Molecular Modeling*, **22**, 1-10 (2016). <https://doi.org/10.1007/s00894-016-2988-y>
5. W. Wang, J. Zhang, W. Qi, R. Su, Z. He, and X. Peng, *ACS Chemical Neuroscience*, **12**(12), 2182-2193 (2021). <https://doi.org/10.1021/acschemneuro.1c00177>
6. P. Singh, N. Jha, and L. Mishra, *Journal of Inorganic and Nuclear Chemistry*, **42**(2), 282-285 (1980). [https://doi.org/10.1016/0022-1902\(80\)80258-2](https://doi.org/10.1016/0022-1902(80)80258-2)

7. P. Ghosh, S. K. Dey, M. H. Ara, K. Karim, and A. Islam, *Egyptian Journal of Chemistry*, **62**(Special Issue (Part 2) Innovation in Chemistry), 523-547 (2019). <https://doi.org/10.21608/ejchem.2019.13741.1852>
8. A. Al-Sarray, *Current Chemistry Letters*, **13**(1), 207-224 (2024). <http://doi.org/10.5267/j.ccl.2023.6.007>
9. A. Mumtaz, T. Mahmud, M. Elsegood, and G. Weaver, *Journal of Nuclear Medicine and Radiation Therapy*, **7**(310), 2 (2016). <http://doi.org/10.4172/2155-9619.1000310>
10. H. M. Salh and T. H. Al-Noor, *Ibn AL-Haitham Journal For Pure and Applied Sciences*, **36**(1), 170-185 (2023). <https://doi.org/10.30526/36.1.2899>
11. H. M. Salh and T. H. Al-Noor, *Journal of Medicinal and Chemical Sciences*, (2023). <https://doi.org/10.26655/JMCHMSCI.2023.7.13s>
12. F. A. Cotton, G. Wilkinson, C. A. Murillo, and M. Bochmann, 'Advanced inorganic chemistry', John Wiley and Sons, Inc., 1999.
13. R. A. Nyquist. *Interpreting Infrared, Raman, and Nuclear Magnetic Resonance Spectra*; Academic Press, 2001
14. W. J. Geary, *Coordination Chemistry Reviews*, **7**(1), 81-122 (1971). [https://doi.org/10.1016/S0010-8545\(00\)80009-0](https://doi.org/10.1016/S0010-8545(00)80009-0)
15. H. Gunther and H. Gunther. 'NMR spectroscopy: Basic principles, concepts, and applications in chemistry', John Wiley & Sons Chichester, UK, 1994
16. A. J. A. Al-Sarray, B. E. Jasim, N. A.-A. Aboud and F. J. Moaen, *Polymer (Korea)*, **48**(2), 188-194 (2024). <http://doi.org/10.7317/pk.2024.48.2.188>
17. K. Nakamoto, 'Infrared and Raman spectra of inorganic and coordination compounds, part B: Applications in coordination, organometallic, and bioinorganic chemistry', John Wiley & Sons, 2009.
18. E. Abdalrazaq, A. A. Q. Jbarah, T. H. Al-Noor, G. T. Shinain, and M. M. Jawad, *Indonesian Journal of Chemistry*, **22**(5), 1348-1364 (2022). <https://doi.org/10.22146/ijc.74020>
19. E. I. Yousif and H. A. Hasan, *Ibn AL-Haitham Journal For Pure and Applied Science*, **30**(1), 73-87 (2017). <https://doi.org/10.30526/30.1.1061>
20. S. Gorelsky, E. Dodsworth, A. Lever and A. Vlcek, *Coordination Chemistry Reviews*, **174**(1), 469-494 (1998). [https://doi.org/10.1016/S0010-8545\(98\)00144-1](https://doi.org/10.1016/S0010-8545(98)00144-1)
21. R. A. Al-Hassani, *International Journal of ChemTech Research*, **9**(5), 723-737 (2016).
22. F. S. Santos, T. M. Costa, V. Stefani, P. F. Goncalves, R. R. Descalzo, E. V. Benvenuti and F. S. Rodembusch, *The Journal of Physical Chemistry A*, **115**(46), 13390-13398 (2011). <https://doi.org/10.1021/jp206905f>
23. B. E. Jasim, A. J. Al-Sarray and R. M. Dadoosh, *Analytical Science and Technology*, **37**(1), 39-46 (2024). <http://doi.org/10.5806/AST.2024.37.1.39>
24. T. H. Al-Noor and L. K. Abdul Kareem, *Ibn Al-Haitham Journal for Pure and Applied Science*, 235-247 (2017). <https://doi.org/10.30526/2017.IHSCICONF.1797>
25. R. M. Silverstein and G. C. Bassler, *Journal of Chemical Education*, **39**(11), 546 (1962). <https://doi.org/10.1021/ed039p546>
26. A. J. Al-Sarray, I. M. H. Al-Mousawi, and T. H. Al-Noor, *Chemical Methodologies*, **6**(4), 331-338 (2022). <https://doi.org/10.22034/chemm.2022.328714.1439>
27. T. H. Al-Noor, A. Mahmood Ali, A. J. Al-Sarray, O. H. Al-Obaidi, A. I. Obeidat, and R. R. Habash, *Journal of University of Anbar for Pure Science*, **16**(1), 20-26 (2022). <https://doi.org/10.37652/juaps.2022.174832>
28. M. Azam, S. I. Al-Resayes, S. M. Wabaidur, M. Altaf, B. Chaurasia, M. Alam, S. N. Shukla, P. Gaur, N. T. M. Albaqami, and M. S. Islam, *Molecules*, **23**(4), 813 (2018). <https://doi.org/10.3390/molecules23040813>
29. T. T. Eugene-Osoikhia, A. Aleem and F. Ayeni, *FUDMA Journal of Sciences*, **4**(2), 217-232 (2020). <https://doi.org/10.33003/fjs-2020-0402-179>
30. Y. Chen and W. Zhang, *Journal of Chemical Crystallography*, **51**, 132-138 (2021). <https://doi.org/10.1007/s10870-020-00828-3>

Authors' Positions

Laith Jumaah Al-Gburi : Graduate Student
Taghreed H. Al-Noor : Professor